

Ultra-Strongly Self-Interacting Dark Matter and the Origin of Little Red Dots

M. Grant Roberts

*Co-Authors: Pierce Giffin, Stefano Profumo, Tesla Jeltema,
Wolfgang Altmannshofer, Aarna Garg*
Email: migrober@ucsc.edu



Physics
UC Santa Cruz

May 12, 2026



From papers:

- ▶ Early formation of supermassive black holes from the collapse of strongly self-interacting dark matter (2410.17480 → JCAP)
- ▶ Little Red Dots from Ultra-Strongly Self-Interacting Dark Matter (2507.03230 → JCAP)
- ▶ Ultra-Strongly Self-Interacting Dark Matter: From Phenomenology to Astrophysical Observables (2510.18142)



The Clustering of Little Red Dots from
Ultra-Strongly Self-Interacting Dark Matter
(2512.18000)



Why SIDM?

- ▶ SIDM solves small scale structure problems: Core-cusp, diversity of rotation curves, and too-big-too-fail.

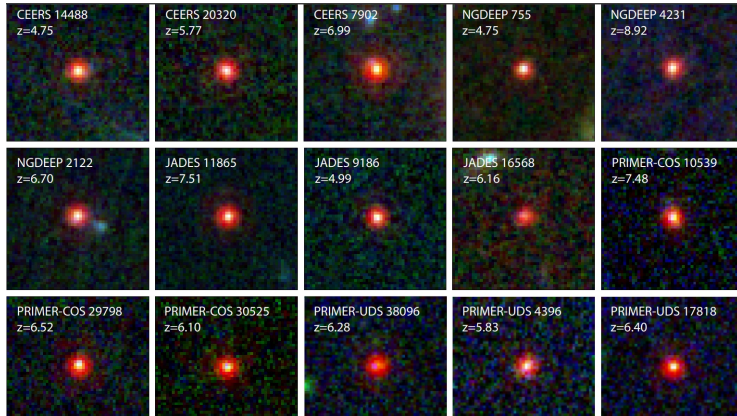
Why uSIDM?

- ▶ Due to very large σ/m ($\sim 10^3 - 10^4$ cm²/g) uSIDM collapses the inner DM halo core into BH seeds, which can grow to the observed high-z quasar and Little Red Dot measurements.

→ SIDM affects the late universe halo structure and uSIDM drives rapid gravothermal collapse of the inner halo core

Little Red Dots from uSIDM

LRDs are a newly observed class of massive, compact ($\lesssim 50 - 100$ pc), high-redshift ($z \gtrsim 5$) AGN that may be $\gtrsim 10 \times$ more numerous than quasars. Images from Kocevski et al 2024 2404.03576





Gravothermal Evolution and Core Collapse

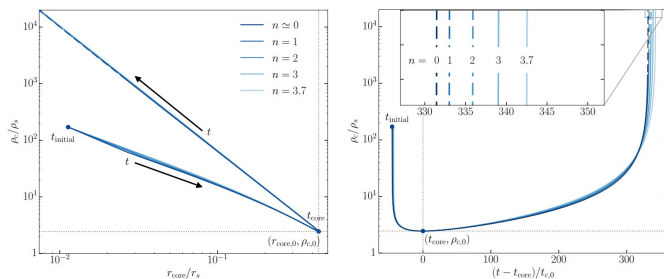


Figure: Building on Pollack et al. 2015, 1501.00017 , we show from Outmezguine et al 2023, 2204.06568, fits to fluid sims

- ▶ SIDM allows heat to flow outward from the dense inner halo.
- ▶ The core first expands, then enters a runaway collapse phase.
- ▶ For $\sigma/m \sim 10^3 - 10^4 \text{ cm}^2/\text{g}$, collapse can occur early enough to form heavy SMBH seeds.



uSIDM Phenomenology

Can we have both SIDM and uSIDM?

→ How can this be constrained?

→ And what are the consequences?

Goal: We want a model where ordinary SIDM remains viable, while a tiny uSIDM fraction collapses early enough to seed SMBHs and LRDs



- ▶ 2 DM particles:
 - ▶ $\chi_1 =$ uSIDM particle
 - ▶ $\chi_2 =$ regular SIDM particle
- ▶ 1 dark photon A'^μ , no portal to the SM

$$\mathcal{L}_{\text{dark}} = \bar{\chi}_1 (i\not{\partial} - m_{\chi_1}) \chi_1 + \bar{\chi}_2 (i\not{\partial} - m_{\chi_2}) \chi_2 - g_{\chi_1} \bar{\chi}_1 A'^\mu \gamma_\mu \chi_1 - g_{\chi_2} \bar{\chi}_2 A'^\mu \gamma_\mu \chi_2 - \frac{1}{4} F'^{\mu\nu} F'_{\mu\nu} - \frac{1}{2} m_{A'}^2 A'^\mu A'_\mu,$$

We also have the conditions that $m_{\chi_1} \gtrsim m_{\chi_2}$, $g_{\chi_2} \sim g_{\chi_1} f_\chi^{1/4}$, and $f_\chi \ll 1$: so to specify the full model, we have 5 free parameters: $\{m_{\chi_1}, m_{\chi_2}, m_{A'}, g_{\chi_1}, f_\chi\}$. f_χ is closely related to f , the fraction of the dark matter that is uSIDM



By expanding $\langle \sigma v \rangle$, we can derive an analytic result for the relationship between $\alpha_{\chi_2} = \frac{g_{\chi_2}^2}{4\pi}$ and m_{χ_2} :

$$\begin{aligned} \left(\frac{m_{\chi_2}}{\text{GeV}}\right) &\sim \frac{\alpha_{\chi_2}}{1.92 \times 10^{-5}} \sqrt{\frac{15}{x_{f_2}}} (1 - \delta), \\ f &\sim f_{\chi} \frac{x_{f_1}}{x_{f_2}} \left(1 - \frac{1}{x_{f_2}} \ln f\right)^2, \\ \delta &\sim 2.81 \times 10^{-7} \left(\frac{f_{\chi}}{10^{-4.1}}\right) \left(\frac{x_{f_1}}{24}\right) \left(\frac{15}{x_{f_2}}\right)^3 \left[\frac{1}{15} \left(\frac{15}{x_{f_2}}\right) - 8 \left(\frac{\ln f}{8}\right)\right]^2. \end{aligned}$$

Thus, the uSIDM particle only introduces a small correction onto the usual SIDM thermal relic relation.

SIDM Observables: Rotation Curves and Galaxy Cluster Strong Lensing

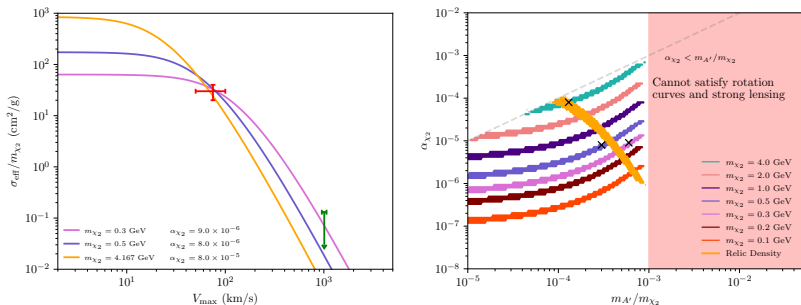


Figure: Rotation curve constraints (accounting for gravothermal evolution) from Roberts et al. 2407.15005 and an upper limit from galaxy cluster strong lensing Andrade et al. 2012.06611. The orange curve corresponds to the derived uSIDM relic density relation.



The LRD Mass Function from uSIDM:

- ▶ We start from seed formation in halos.
- ▶ We then grow the seeds via a log-normal distribution of sub-Eddington accretion rates, $\lambda_0 \approx 0.2$ and dispersion $\sigma_\lambda \approx 0.3$.
- ▶ Apply a duty cycle of $\varepsilon_{\text{DC}} = 0.01$.

$$\frac{dN_{\text{BH}}^{\text{seed}}}{d \log_{10} m_{\text{BH}}^{\text{seed}}} = \ln 10 \frac{dN_{\text{BH}}^{\text{seed}}}{dN_H} \frac{dN_H}{d \ln m_{200}} \frac{m_{\text{BH}}^{\text{seed}}}{m_{200}} \frac{dm_{200}}{dm_{\text{BH}}^{\text{seed}}},$$

$$\frac{d^2 N_{\text{BH}}^{\text{grow}}}{d \log_{10} m_{\text{BH}} d\lambda} = \varepsilon_{\text{DC}} P(\lambda) \frac{dN_{\text{BH}}^{\text{seed}}}{d \log_{10} m_{\text{BH}}^{\text{seed}}}$$

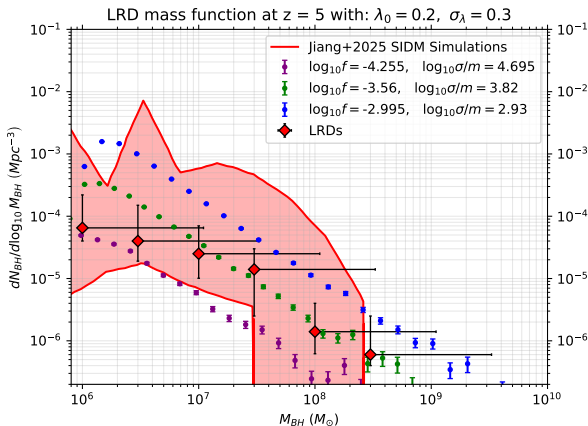


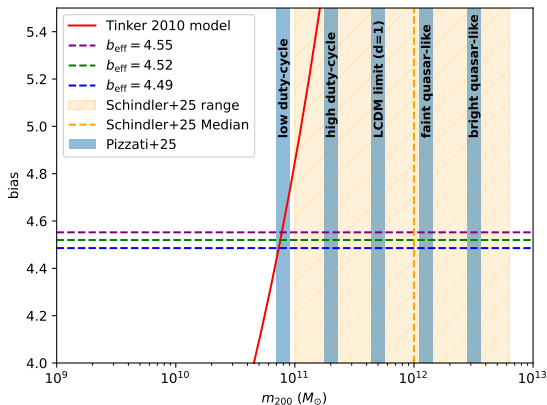
Figure: We show the uSIDM LRD mass function (colored dots) for different uSIDM parameters taken from Fig. 3 in Roberts et al 2507.03230, plotted against the SIDM simulation results from Jiang et al 2503.23710 (shaded red), and the LRD mass function data points from Kokorev et al 2401.09981 (red-diamonds).



The halo bias, b_h , is the relation between the two-point dark matter halo correlation function, and the two-point matter correlation function: $\xi_{hh} \simeq b_h^2 \xi_{mm}$. For LRDs, we infer an effective clustering bias, b_{eff} : $\xi_{\text{LRD, LRD}} \simeq b_{\text{eff}}^2 \xi_{mm}$,

$$b_{\text{eff}} = \langle b_h(m_{200}, z) \rangle_{\text{LRD, hosts}}$$

$$b_{\text{eff}} = \frac{\int d \log_{10} m_{200} \phi_{\text{LRD}}(m_{\text{BH}}) \frac{d \log_{10} m_{\text{BH}}}{d \log_{10} m_{200}} b_h[m_{200}, z]}{\int d \log_{10} m_{200} \phi_{\text{LRD}}(m_{\text{BH}}) \frac{d \log_{10} m_{\text{BH}}}{d \log_{10} m_{200}}}$$



Our three fiducial parameters yield $b_{\text{eff}} \sim 4.52 \pm 0.03$, and infer host-halo masses around $8 \times 10^{10} M_{\odot}$, which is the first LRD clustering prediction to date. Therefore, uSIDM predicts that LRDs occupy a distinct host-halo population from high- z quasars



We have found that:

- ▶ A small fraction of uSIDM can rapidly core-collapse to form BH seeds, while the dominant SIDM component remains consistent with observational bounds.
- ▶ The uSIDM LRD mass function is a good match for the observations.
- ▶ uSIDM clustering predicts LRDs to be a distinct population from high- z quasars, with $b_{\text{eff}} \sim 4.5$, which should be testable with upcoming JWST measurements.

Future works:

- ▶ Can the uSIDM model impact other LRD special features, such as X-ray quietness?
- ▶ Milky Way scale constraints on SIDM σ/m from uSIDM σ/m ?
- ▶ Including Dark Bondi accretion can preserve agreement with observables while modifying growth histories.



Thank you for listening, do you have any questions?





Backup Slides

SIDM and uSIDM cross-section comparison

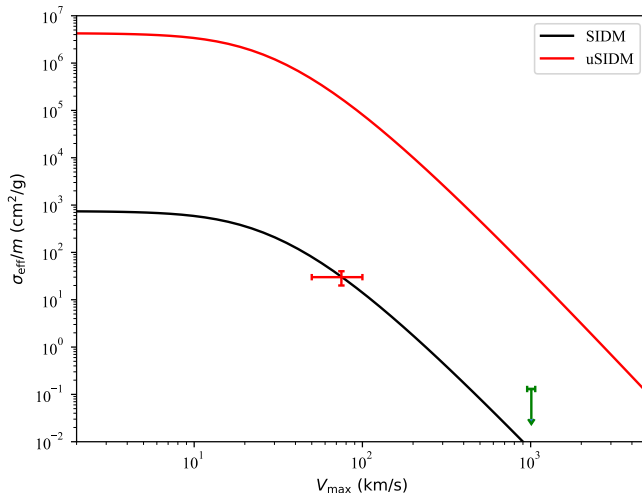
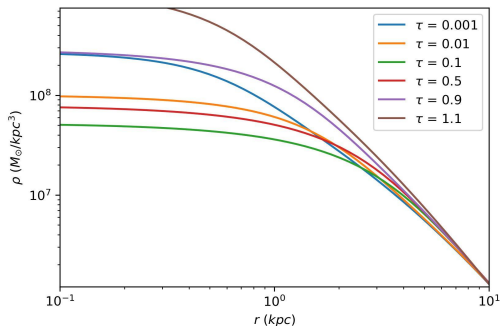


Figure: Using the relic density parameters (the orange curve)

→ Gravo-thermal Evolution and Core Collapse



While the above theory curves are very helpful, here is a plot that shows how this physically changes the dark matter density profile:

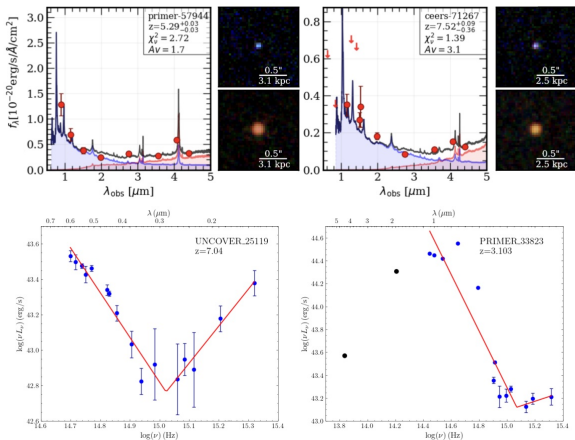


τ is a dimensionless time parameter which I will explain in more detail later, but $\tau = 0$ is the initial starting configuration for the halo

LRD Spectral Energy Distribution



They have an interesting property of a “v-shaped” spectral energy distribution. The top is from Kokorev et al 2024 2401.09981 and bottom is from Zhang et al 2025 2505.12719





Data Set:

From the SPARC data set, we chose 10 galaxies: DDO 154, ESO 444-G084, F568-V1, F574-1, NGC 0300, NGC 3109, UGC 00128, UGC 06446, UGC 06667, and UGC 08286

From the Relatores et al 2019 data set, we chose 4 galaxies: NGC 4376, NGC 4396, NGC 7320, and UGC 4169

The criteria for our chosen galaxies was that they needed to all be similarish in V_{max} , and that they needed to be dark matter dominated at their innermost measured data point, typically $r < 0.5 - 1$ kpc for SPARC, but $r \leq 0.5$ kpc for Relatores

Galaxy Rotation Curves

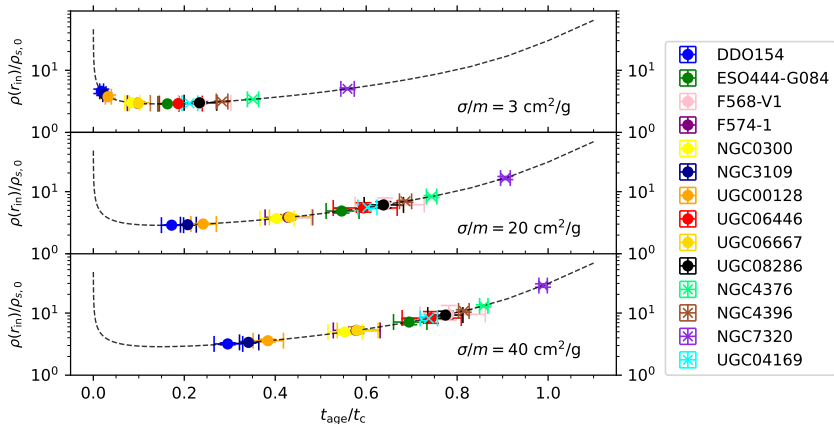


Figure: Fits from Roberts et al 2024, 2407.15005

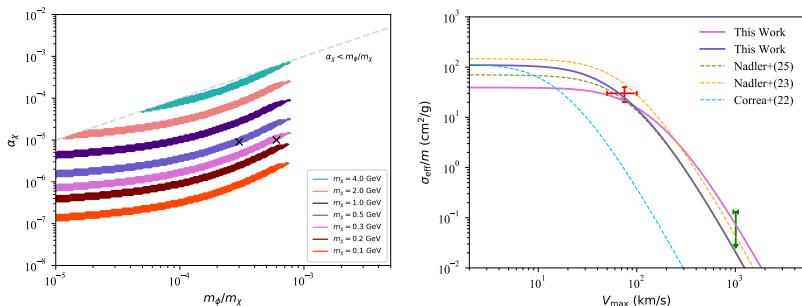


Figure: Left panel: Favored parameter regions where the effective SIDM cross section satisfies the following conditions simultaneously: $\sigma_{\text{eff}}/m = 20\text{--}40$ cm²/g at $V_{\text{max}} = (75 \pm 25)$ km/s, and $\sigma_{\text{eff}}/m < 0.13$ cm²/g at $V_{\text{max}} = (1000 \pm 55)$ km/s. Right panel: Effective cross sections as a function of V_{max} for the cases $m_\chi = 0.3$ GeV (pink) and 0.5 GeV (purple).



Instabilities of metal-poor gas clouds

These clouds are unstable enough to allow for collapse into a BH rather than fragmentation into forming stars first. While these directly form BHs, the mass range is $m_{\text{BH}}^{\text{seed}} \approx 10^4 M_{\odot}$, which requires long phases of Eddington or super-Eddington accretion, and as we just discussed, has several problems

Stellar-dynamical methods

As early primordial gas becomes enriched with heavy elements via Pop III stars, the next generation of stars form. If there is a sufficiently dense population of low mass stars, they can form nuclear star clusters where runaway stellar mergers grow the stars into large enough objects that then collapse into BHs with $m_{\text{BH}}^{\text{seed}} \approx 10^2 - 10^4 M_{\odot}$. Unfortunately, as the metallicity of the gas increases, this process becomes less efficient



Mergers

While simulations have shown that mergers are the primary mechanism of growth for high-redshift BHs, this is highly dependent on the formation of heavy seeds and their distributions. However, velocity kicks can slingshot one of the merging BHs out of the system entirely, hence ending the growth cycle of the primary BH seed. The merger process also may not occur fast enough to match observations

→ Because of these issues, we elected to explore the possibility of gravothermally collapsing dark matter halos into SMBH seeds much earlier, which can then grow via accretion within the observational limits



First, we compute the collapse redshift, z_{coll} , for forming the BH seed from gravothermal collapse of the halo:

$$t(z_{\text{coll}}) - t(z_{\text{vir}}) = 455.65 t_{\text{rel}}(f, \sigma/m, m_{200}, z_{\text{vir}}, c_{200}), \quad (1)$$

where the relax time, t_{rel} , is defined as

$$t_{\text{rel}}(f, \sigma/m, m_{200}, z, c_{200}) = 0.354 \text{ Myr} \left(\frac{m_{200}}{10^{12} M_{\odot}} \right)^{-1/3} \left(\frac{k_c(c_{200})}{k_c(9)} \right)^{3/2} \\ \times \left(\frac{c_{200}}{9} \right)^{-7/2} \left(\frac{\rho_{\text{crit}}(z)}{\rho_{\text{crit}}(z=15)} \right)^{-7/6} \left(\frac{f\sigma/m}{1 \text{ cm}^2/\text{g}} \right)^{-1}, \quad (2)$$

with $k_c(x) = \ln(1+x) - x/(1+x)$ and $\rho_{\text{crit}}(z)$ the critical density of the universe at a given redshift.



The time is given in the typical way,

$$t(z) = \int_z^\infty \frac{dz'}{(1+z')H(z')}, \quad (3)$$

with $H(z)$, the Hubble rate. From Pollack et al 2015, they ran simulated halos to infer how much of the inner core would fully collapse into the BH seed, they found that a typical amount of about 2.5% of m_{200} would turn into the seed, which sets the normalization for their estimate of the BH seed formation mass:

$$\frac{m_{\text{BH}}(z)}{m_{200}} \sim \frac{0.025f}{\ln(1+c_{200}) - \frac{c_{200}}{1+c_{200}}}. \quad (4)$$



Once the seed has formed, we grow the seed via accretion to an observed quasar redshift, z_{obs} . We control the accretion rate by parameterizing it to the number of e-folds of accretion (N_e) during which the SMBH grows, as:

$$t(z_{\text{obs}}) = t(z_{\text{coll}}) + N_e t_{\text{sal}}, \quad (5)$$

where t_{sal} is the Salpeter time; which is the time scale it would take a BH to double its mass via Eddington accretion and is given by,

$$t_{\text{sal}} = \frac{\epsilon_r \sigma_{TC}}{4\pi G m_p} \approx \left(\frac{\epsilon_r}{0.1} \right) 45.1 \text{ Myr}. \quad (6)$$

Following the literature, we set $\epsilon_r = 0.1$. The seed then grows exponentially as: $m_{\text{BH}}^{\text{theory}}(z_{\text{obs}}) = m_{\text{BH}}^{\text{seed}}(z_{\text{coll}}) \exp(N_e)$.

Backup Slide: Seeding SMBHs via uSIDM



The full 8 quasar sample:

Quasar	$\log_{10} M. (M_{\odot})$	z
J0100+2802	10.29	6.327
	10.09	6.316
	10.33	6.300
J0842+1218	9.404	6.075
	9.300	6.067
	9.520	6.070
	9.230	6.069
P007+04	9.356	6.002
	9.890	5.954
	9.910	5.980
P036+03	9.775	6.541
	9.430	6.527
P183+05	9.674	6.439
	9.410	6.428
P231-20	9.806	6.587
	9.520	6.564
P323+12	9.243	6.587
	8.920	6.000
P359-06	9.577	6.172
	9.000	6.169



Backup Slide: uSIDM Power-law fit

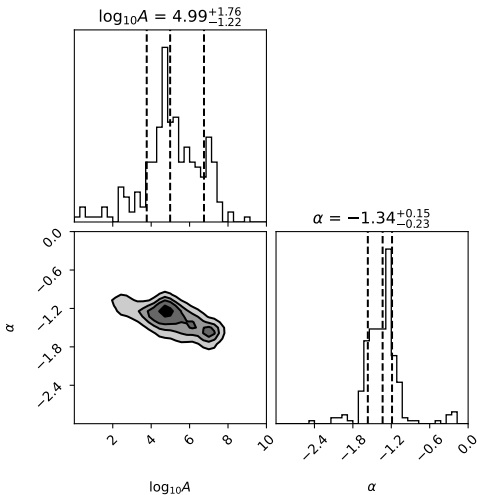


Figure: Power-law fit: $\frac{dN_{BH}}{d \log_{10} m_{BH}} = A m_{BH}^{\alpha}$



$$\sigma_V = \frac{3}{2} \int d \cos \theta \sin^2 \theta \frac{d\sigma}{d \cos \theta} \quad (7)$$

$$\frac{d\sigma}{d \cos \theta} = \frac{\sigma_0 w^4}{2 [w^2 + v^2 \sin^2 (\theta/2)]^2} \quad (8)$$

$$\sigma_V = \frac{6\sigma_0 w^6}{v^6} \left[\left(2 + \frac{v^2}{w^2} \right) \ln \left(1 + \frac{v^2}{w^2} \right) - \frac{2v^2}{w^2} \right] \quad (9)$$

$$\sigma_{\text{eff}} = \frac{2 \int v^2 dv d \cos \theta \frac{d\sigma}{d \cos \theta} v^5 \sin^2 \theta \exp \left[-\frac{v^2}{4(\sigma_{1D})^2} \right]}{\int v^2 dv d \cos \theta v^5 \sin^2 \theta \exp \left[-\frac{v^2}{4(\sigma_{1D})^2} \right]} \quad (10)$$

$$\sigma_{\text{eff}} \approx \frac{1}{512 (\sigma_{1D})^8} \int v^2 dv \frac{2}{3} \sigma_V v^5 \exp \left[-\frac{v^2}{4 (\sigma_{1D})^2} \right] \quad (11)$$

where $\sigma_0 = 4\pi\alpha_\chi^2 / (m_\chi^2 w^4)$ and $w = m_\phi c / m_\chi$